Two-Dimensional Melting under Quenched Disorder

Sven Deutschländer,[1] Tobias Horn,[2] Hartmut Löwen,[2] Georg Maret,[1] and Peter Keim[1]

[1]*Fachbereich für Physik, Universität Konstanz, D-78464 Konstanz, Germany*
[2]*Institut für Theoretische Physik II: Heinrich-Heine-Universität Düsseldorf, D-40225 Düsseldorf, Germany*
(Received 10 May 2013; published 27 August 2013)

We study the influence of quenched disorder on the two-dimensional melting behavior of super-paramagnetic colloidal particles, using both video microscopy and computer simulations of repulsive parallel dipoles. Quenched disorder is introduced by pinning a fraction of the particles to an underlying substrate. We confirm the occurrence of the Kosterlitz-Thouless-Halperin-Nelson-Young scenario and observe an intermediate hexatic phase. While the fluid-hexatic transition remains largely unaffected by disorder, the hexatic-solid transition shifts to lower temperatures with increasing disorder. This results in a significantly broadened stability range of the hexatic phase. In addition, we observe spatiotemporal critical (like) fluctuations, which are consistent with the continuous character of the phase transitions. Characteristics of first-order transitions are not observed.

Since the seminal work of Kosterlitz, Thouless [1,2], Halperin, Nelson, and Young (KTHNY) [3–5] it has been known that melting in two spatial dimensions can be qualitatively different from three-dimensional bulk melting. While the latter is typically a phase transition of first order, a two-stage scenario with an intervening hexatic phase can emerge in two-dimensional systems, which is separated from the isotropic fluid and solid phase by two continuous transitions [6]. The KTHNY melting scenario further predicts that, in two dimensions, the melting process is mediated by the unbinding of thermally activated topological defects. In particular, the emergence of the hexatic phase is related to the dissociation of dislocation pairs into isolated dislocations [2,7]. These break translational symmetry, leading to a vanishing shear modulus. However, the orientational symmetry remains quasi long range and the modulus of rotational stiffness, Frank's constant K_A, attains a nonvanishing value [4]. It has been shown that the KTHNY scenario is realized for soft long-range pairwise potentials scaling with the inverse cube of the particle separation [8,9]. In fact, video microscopy experiments with superparamagnetic colloidal particles pending at a two-dimensional air-water interface and exposed to an external magnetic field perpendicular to the interface have confirmed the KTHNY scenario in detail [10–12]. Further reports on soft repulsive particles in two dimensions are in favor of the KTHNY scenario [13–15] while in systems with very short-ranged or hard-core particle interactions, first-order characteristics were found for both transitions [16,17]. Here, we investigate whether the continuous melting including critical fluctuations persists in the presence of quenched disorder or whether first-order signatures emerge instead [18].

Pure 2D bulk systems are rare in nature; planar confinement is typically realized by adsorption on an interface, such that crystallization usually occurs on solid substrates

(examples include graphene sheets, see Ref. [19]) which introduce quenched (i.e., frozen-in) disorder due to some roughness. The same holds for flux lines pinned by impurities [20–23], which leads to large critical fields in type II superconductors. Defects may also affect the phase behavior of freely suspended liquid crystal films [24], of synthetic [25] and biological [26] Langmuir Blodgett films, or even 2D protein crystals [27]. Based on a topological defect analysis for weak disorder, Nelson and co-workers [28,29] have predicted that the KTHNY scenario persists with a widening of the hexatic stability range for increasing strength of quenched disorder. This notion was questioned in subsequent theoretical studies [30]. More recent experimental efforts [31–34], simulations [35–37], and theories [38] have markedly increased our understanding of two-dimensional melting under disorder, but the occurrence of the hexatic phase was never resolved in all of these studies. Therefore, the above-mentioned predictions of Nelson and co-workers [28,29] have never been tested by experiment or simulations.

In this Letter, we propose an experiment on superparamagnetic colloids on a glass substrate on which a small fraction of the particles is pinned, inducing quenched disorder. Clearly, as a reference, the KTHNY scenario occurs for the pure case without any disorder on a pinning-free air-water interface [10,12]. We can now systematically study the melting scenario in detail for different fractions of pinned particles. In our experiments, we confirm the KTHNY scenario and the predictions by Nelson and co-workers [28,29] under disorder. The stability range of the hexatic phase widens upon increasing disorder as opposed to the prediction of Ref. [30]. We also perform two-dimensional computer simulations for parallel dipoles and find good agreement with our experimental data. Extracting an "effective" K_A, we recover the scaling of the elasticity modulus in the presence of disorder. Thereby,

we provide evidence that melting in the presence of disorder is governed by the same defect-mediated process predicted and confirmed for pure systems. Furthermore, we observe heterogeneous orientational order close to the melting temperature but a long-time analysis reveals that such heterogeneities fluctuate strongly on time scales larger than the orientational correlation time indicating critical behavior.

The experimental system consists of superparamagnetic colloidal particles which are confined in two dimensions and subject to quenched disorder embodied by a random distribution of fixed particles. The colloidal suspension is kept at room temperature and an external magnetic field H applied perpendicular to the particle layer induces a repulsive dipole-dipole potential $V(r) = \mu_0(\chi H)^2/r^3$, where χ denotes the magnetic susceptibility [39] and r the particle distance. The phase behavior is studied by tuning the interaction strength via the external magnetic field, quantified by the dimensionless interaction parameter

$$\Gamma = \frac{\mu_0(\pi n)^{3/2}(\chi H)^2}{k_B T}, \quad (1)$$

with the 2D particle density n and the thermal energy $k_B T$. The particles have a diameter $d = 4.5$ μm and the mass density 1.7 kg/dm^3. The suspension is sealed within a cell consisting of two parallel cover slips glued together via a hollow cylindrical glass spacer of 5 mm diameter. By gravity, the particles sediment and form a monolayer on the bottom glass plate, where a short-time lateral diffusion constant of $D = 0.0295$ μm^2/s is observed. Because of van-der-Waals interactions and chemical reactions between colloids and the glass surface, a small amount of particles pin to the substrate. This distribution is slowly altered by thermal tearing or the creation of new pinning connections, but the pinned particles are fixed on the time scale of our measurements. We exemplify three different sample regions with varying pinning strengths ranging from approximately 0.5% to 0.8%. The colloidal ensemble is melted from an equilibrated crystalline state by decreasing H in small steps. After each step, the system is allowed to equilibrate for at least 24 hours before particle trajectories are recorded via video microscopy [40] for 2.7 hours, which equals $\approx 50\tau_B$.

Complementary, computer simulations are carried out in the NAT ensemble, with A denoting the area of the system. The total particle number is fixed to $N = 16000$ and periodic boundary conditions are applied. Each pinning strength is sampled with at least 15 statistically independent configurations of obstacles, which are achieved by pinning randomly selected particles in a fluid configuration of hard disks at a packing fraction of 0.25%. Within statistical precision, this realization of pinning corresponds to the distribution of pinned particles observed in the experiment. Using the standard Metropolis Monte Carlo (MC) algorithm, a full freezing and melting cycle is

conducted for each particular setup at which the initially chosen particles remain pinned. After incrementing $\Gamma \propto 1/T$, the system is equilibrated for 5×10^5 MC sweeps before recording data. While Monte Carlo methods are known to converge rapidly towards static equilibrium states, the underlying phase-space sampling provides a suitable means to study dynamic properties, as well [41]. For each parameter set of temperature and pinning strength, the observables obtained by MC simulations are averaged over all sample realizations of disorder.

The KTHNY theory predicts a two-step melting process, in which the isotropic fluid and solid phase are separated by an intermediate hexatic phase. While translational order is only short range in the hexatic phase, orientational order persists. More precisely, it switches from long range in the solid over quasi long range in the hexatic phase to short range in the isotropic fluid. The characteristic range of orientational order in the different phases can be quantified in terms of the correlation $g_6(r, t)$ of the bond order parameter

$$\psi_6 = \frac{1}{n_j}\sum_k e^{i6\theta_{jk}}, \quad (2)$$

where the sum goes over all n_j nearest neighbors of particle j, and θ_{jk} is the angle of the kth bond in respect to a certain reference axis. Mapping the characteristic ranges of the spatial orientational order on the time domain, we can study the dynamical orientational correlation $g_6(t) = \langle \psi_6^*(t)\psi_6(0)\rangle$, which, analogously to the spatial correlation, decays exponentially in the isotropic fluid, and algebraically in the hexatic phase, and approaches a constant value in the solid [42]. This quantity is well suited to characterize the melting process, as discussed in Refs. [8,9] and successfully employed experimentally in Ref. [10].

Figure 1 shows $g_6(t)$ for both, experiment (0.48% pinning) and simulation (0.5%). The time axis is reduced to the Brownian time scale $\tau_B = (d/2)^2/D$. After a short-time decay due to Brownian motion, the characteristic behavior of the solid, the hexatic (linear decay in the log-log plot), and isotropic fluid is clearly distinguishable at long times. To confirm the characteristic decay behavior, $g_6(t)$ is fitted with a second-order polynomial fit on a double-logarithmic scale: $\ln(g_6(t)) = a + b\ln(t/\tau_B) + c\ln^2(t/\tau_B)$, with dimensionless coefficients a, b, and c. Solid, hexatic, and isotropic fluid phases are characterized by the relative contribution of positive or negative curvature, expressed by $c/|b|$. We define an upper and a lower threshold value for $c/|b|$ to distinguish between the negatively curved exponential decay of $g_6(t)$ in the isotropic fluid, positive curvature in the solid, and a linear course in between, reflecting the hexatic phase (for further details and an evaluation of the spatial bond order correlation function see the Supplemental Material [43]).
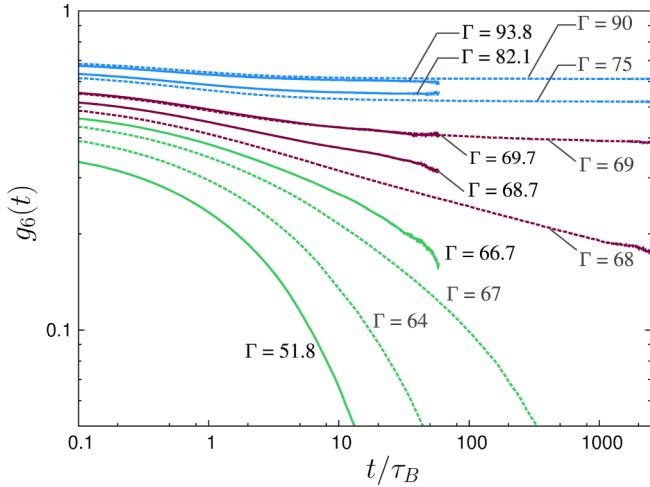
FIG. 1 (color online).   Temporal bond orientational correlation function $g_6(t)$ in the presence of quenched disorder plotted versus reduced time t/τ_B on a double-logarithmic scale. The fraction of pinned particles is 0.48% in the experiment and 0.5% in the simulation. Exemplary curves are shown for the isotropic fluid [green (light gray)], hexatic [red (black)], and solid [blue (dark gray)] phase, where experimental data are drawn with solid lines, and computer simulations with dashed lines.

To illustrate the critical behavior at the transition points, we determine the orientational correlation time ξ_t and an "effective" Frank's constant K_A, characterizing the elastic response of topological defects to torsion in the presence of pinned particles (see Fig. 2). The parameters are extracted from exponential fits $\sim e^{-t/\xi_t}$ in the isotropic fluid and algebraic fits $\sim t^{\eta_6/2}$ in the hexatic phase, where the orientational exponent $\eta_6 = 18k_BT/\pi K_A$ is inversely proportional to Frank's constant. In the isotropic fluid, K_A is zero due to the appearance of isolated disclinations. The
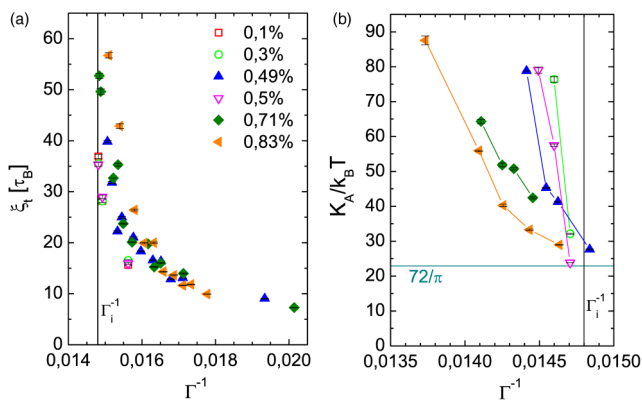
corresponding stress field "absorbs" external torsion by diffusion and/or rotation. Approaching the hexatic-isotropic fluid transition at the temperature $\Gamma_i^{-1} \approx 0.0148$, ξ_t diverges, and K_A jumps to the finite value $72/\pi$. In the hexatic phase, K_A remains constant due to the presence of quasi–long-range orientational order: a torsion would mediate a separation of dislocations into isolated disclinations, inducing a change in the strain field at a finite stress response. Approaching the solid-hexatic transition, the elastic response to a torsion increases due to the decreasing number of isolated dislocations. Simultaneously, K_A diverges. Our data indicate that, in the presence of disorder, the divergent behavior of Frank's constant spreads. More precisely, K_A increases at lower temperatures for higher pinning strengths, which means that the hexatic-solid transition temperature Γ_m^{-1} strongly depends on disorder, as proposed in Refs. [28,29,35]. Furthermore, this implies the reduction of torsional stiffness at a fixed temperature: in the presence of pinned particles, the response to a torsional stimulus becomes more elastic.

To emphasize the consequences of these distinct characteristics at the transitions on the phase behavior of the system, the two-step melting process is mapped to the parameter plane of temperature and pinning strength. Figure 3 shows the resulting phase diagram. In the cooling and heating cycle of the simulations no hysteresis was found, as is typical for continuous transitions—see the Supplemental Material [43] for details and additional evaluation of our data indicating the continuous nature of the phase transition. The hexatic-isotropic fluid transition is found to remain largely unaffected by pinning; the transition temperature Γ_i^{-1} is barely shifted by disorder. In contrast, the hexatic-solid phase boundary is strongly

FIG. 2 (color online).   (a) Orientational correlation time ξ_t and (b) Frank's constant K_A, for different concentrations of pinned particles. Filled symbols represent experimental data, open symbols simulation. The meaning of the symbols is the same in (a) and (b); lines are guides to the eye. While ξ_t is almost not affected by different pinning strengths, K_A is clearly lowered with increasing pinning.
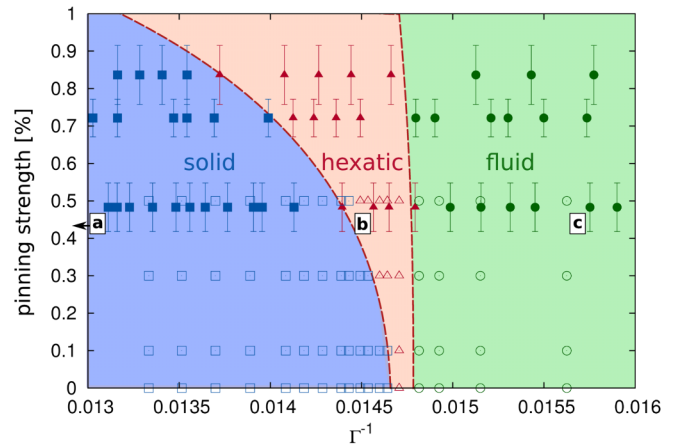

FIG. 3 (color online).   Phase diagram indicating the solid [blue (dark gray)], hexatic [red (light gray)] and isotropic fluid [green (medium gray)] phase in the parameter space of temperature $\propto \Gamma^{-1}$ and pinning strength. Full symbols represent experimental data, while open symbols correspond to simulation results. Letters indicate the location of snapshots in Fig. 4.

influenced. The transition temperature is shifted significantly towards lower values for increasing numbers of pinned particles. This can be explained qualitatively considering the influence of pinned sites on the distinct symmetries: a pinned particle causes a strain field in its vicinity and therefore shifts particles to release the created stress. Orientational order can be recovered, since particles are able to adjust the orientational field ψ_6 to their local environment by slight displacements. However, the hexatic-solid transition is governed by a significant change in translational order. If pinned particles are displaced from their ideal lattice position, a positional lack can only be restored by bending lattice lines. Moreover, the shear modulus is zero in the isotropic fluid and hexatic phase, which disburdens the conservation of order by adjusting the strain. As a result, the stability range of the hexatic phase widens with increasing disorder, which is in accordance with theoretical predictions [28,29]. In addition, this effect seems to become more crucial for higher disorder strengths, resulting in a curved behavior of the hexatic-solid phase boundary. This suggests the existence of a critical disorder strength, above which the system is not able to form an ordered state [35], but rather becomes an amorphous solid in the form of a hexatic glass [31,33], depending on the range of quenched disorder [38].

To determine the dynamics of the orientational order in space, we illustrate the magnitude and spatial distribution of the orientational order parameter $\langle|\psi_6|\rangle_t$, averaged over a finite time window of $\approx 50\tau_B$ [see Figs. 4(a)–4(c)]. In the solid phase, orientational order is homogeneous and persistent in time. It is only locally reduced by thermally activated, short living dislocation pairs. In the hexatic and isotropic fluid phase, the magnitudes of $\langle|\psi_6|\rangle_t$ decrease and are subject to a strongly heterogeneous spatial pattern on various length scales. This behavior can equally be observed in computer simulation snapshots (see the Supplemental Material [43]). Similar heterogeneities were reported for an impurity-free two-dimensional Lennard-Jones system [44]. The observed heterogeneities of the orientational order field close to Γ_i are spatiotemporal and reflect criticallike fluctuations at the hexatic-isotropic fluid transition, thus confirming our finding that this transition is continuous [see movie 1 and 2 in the Supplemental Material [43] covering a time window two decades larger (up to $\approx 4000\tau_B$) compared to Figs. 4(a)–4(c)].

To exhibit the proximate effects of the pinned sites, we compare the spatial dynamics of particles in the vicinity of and far away from pinning centers for an intermediate pinning strength [see Fig. 4(d)]. While in the isotropic fluid the mean square displacement is decreased near pinning, it is increased in the solid. The inhibited dynamics in the disordered phase can be explained by the confining character of the pinned sites. Conversely, the local dynamics in the solid seems to be increased near pinning. This might be
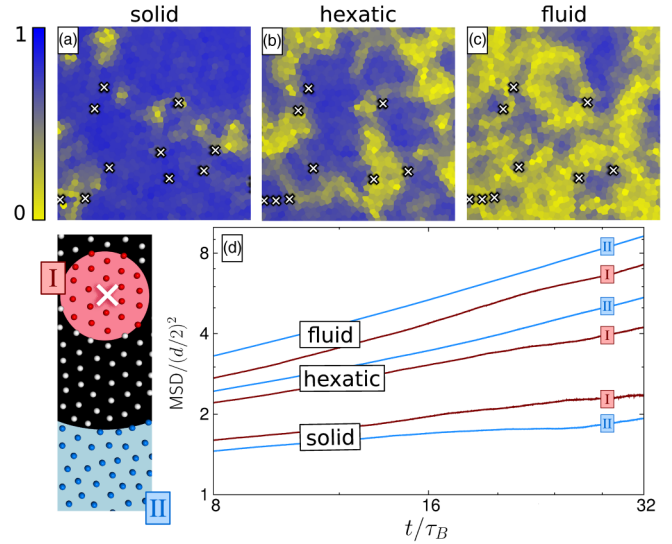

FIG. 4 (color online). (a)–(c) Snapshots of the experimental system at 0.48% pinning, showing the local orientational order parameter $\langle|\psi_6|\rangle_t$ averaged over $\approx 50\tau_B$ in the different phases [(a) $\Gamma^{-1} = 0.0117$, (b) $\Gamma^{-1} = 0.0143$, (c) $\Gamma^{-1} = 0.0154$]. The field of view is $450 \times 450~\mu$m. Voronoi cells are color coded according to the bar on the left. (d) Mean square displacement (MSD) calculated for particles within a distance of $8d$ around pinning sites (region I in the inset) and more than $24d$ away from them (region II). Temperatures correspond to (a)–(c).

related to an increased probability of dislocation pair unbinding induced by quenched disorder [28,35]. The crossover lies in the hexatic phase at $\Gamma^{-1} \approx 0.0144$, close to the solid-hexatic phase transition, which supports our finding that this transition is more affected by quenched disorder than the hexatic-isotropic liquid one.

In conclusion, we investigated the melting transition of 2D crystals under quenched disorder in the form of pinning sites. Analyzing the dynamics of the orientational correlation, we probed the disorder vs temperature phase diagram and determined the orientational correlation time and Frank's constant. Both show divergent behavior at the corresponding phase transition, confirming the continuous melting character of the KTHNY scenario. While the hexatic-isotropic fluid transition is rather unaffected by pinning, the transition from the solid to the hexatic phase is strongly influenced, resulting in a significant broadening of the hexatic phase. In addition, we observed spatiotemporal dynamical heterogeneities of the orientational order parameter (see the movies in the Supplemental Material [43]), marking critical(like) fluctuations, whereas first-order characteristics are not observed. In comparison to the bulk, the local dynamics of particles in the vicinity of pinned sites is decreased in the isotropic liquid, which is not directly reflected by a localization of the fluctuations of the order parameter (see the movies in the Supplemental Material [43]). The further investigation of 2D systems with this kind of weak quenched disorder might reveal

the role of critical fluctuations in the disorder-mediated melting process and also opens the field of hexatic membranes with adatoms or molecules. Using weak random potentials or (quasi)crystalline structures, commensurable and incommensurable crystal transitions come into focus, and for strong disorder, crystal to amorphous solid transitions can be investigated.

[1] J. M. Kosterlitz and D. J. Thouless, J. Phys. C **5**, L124 (1972).
[2] J. M. Kosterlitz and D. J. Thouless, J. Phys. C **6**, 1181 (1973).
[3] B. I. Halperin and D. R. Nelson, Phys. Rev. Lett. **41**, 121 (1978).
[4] D. R. Nelson and B. I. Halperin, Phys. Rev. B **19**, 2457 (1979).
[5] A. P. Young, Phys. Rev. B **19**, 1855 (1979).
[6] K. J. Strandburg, Rev. Mod. Phys. **60**, 161 (1988).
[7] For a review, see P. M. Chaikin and T. C. Lubensky, *Principles of Condensed Matter Physics* (Cambridge University Press, Cambridge, England, 1995).
[8] S. Z. Lin, B. Zheng, and S. Trimper, Phys. Rev. E **73**, 066106 (2006).
[9] N. Gribova, A. Arnold, T. Schilling, and C. Holm, J. Chem. Phys. **135**, 054514 (2011).
[10] K. Zahn and G. Maret, Phys. Rev. Lett. **85**, 3656 (2000).
[11] H. H. von Grünberg, P. Keim, K. Zahn, and G. Maret, Phys. Rev. Lett. **93**, 255703 (2004).
[12] P. Keim, G. Maret, and H. H. von Grünberg, Phys. Rev. E **75**, 031402 (2007).
[13] Y. Han, N. Y. Ha, A. M. Alsayed, and A. G. Yodh, Phys. Rev. E **77**, 041406 (2008).
[14] S. Prestipino, F. Saija, and P. V. Giaquinta, Phys. Rev. Lett. **106**, 235701 (2011).
[15] Y. Peng, Z. Wang, A. M. Alsayed, A. G. Yodh, and Y. Han, Phys. Rev. Lett. **104**, 205703 (2010).
[16] A. H. Marcus and S. A. Rice, Phys. Rev. Lett. **77**, 2577 (1996).
[17] E. P. Bernard and W. Krauth, Phys. Rev. Lett. **107**, 155704 (2011).
[18] Since correlation lengths diverge exponentially in the KTHNY theory such that one can take derivatives arbitrarily often, those transitions are called continuous.
[19] J. C. Meyer, A. K. Geim, M. I. Katsnelson, K. S. Novoselov, T. J. Booth, and S. Roth, Nature (London) **446**, 60 (2007).
[20] A. I. Larkin, Sov. Phys. JETP **31**, 784 (1970).
[21] Y. Imry and S.-K. Ma, Phys. Rev. Lett. **35**, 1399 (1975).
[22] A. I. Larkin and Y. N. Ovchinnikov, J. Low Temp. Phys. **34**, 409 (1979).
[23] D. S. Fisher, M. P. A. Fisher, and D. A. Huse, Phys. Rev. B **43**, 130 (1991).
[24] R. Geer, T. Stoebe, C. C. Huang, R. Pindak, J. W. Goodby, M. Cheng, J. T. Ho, and S. W. Hui, Nature (London) **355**, 152 (1992).
[25] R. Viswanathan, L. L. Madsen, J. A. Zasadzinski, and D. K. Schwartz, Science **269**, 51 (1995).
[26] I. R. Peterson, R. Steitz, H. Krug, and I. Voigt-Martin, J. Phys. (France) **51**, 1003 (1990).
[27] B. Berge, L. Faucheux, K. Schwab, and A. Libchaber, Nature (London) **350**, 322 (1991).
[28] D. R. Nelson, Phys. Rev. B **27**, 2902 (1983).
[29] S. Sachdev and D. R. Nelson, J. Phys. C **17**, 5473 (1984).
[30] R. A. Serota, Phys. Rev. B **33**, 3403 (1986).
[31] R. E. Kusner, J. A. Mann, and A. J. Dahm, Phys. Rev. B **49**, 9190 (1994).
[32] A. Pertsinidis and X. S. Ling, Phys. Rev. Lett. **100**, 028303 (2008).
[33] P. Yunker, Z. Zhang, and A. G. Yodh, Phys. Rev. Lett. **104**, 015701 (2010).
[34] P. Hartmann, A. Douglass, J. C. Reyes, L. S. Matthews, T. W. Hyde, A. Kovacs, and Z. Donko, Phys. Rev. Lett. **105**, 115004 (2010).
[35] M.-C. Cha and H. A. Fertig, Phys. Rev. Lett. **74**, 4867 (1995).
[36] S. Herrera-Velarde and H. H. von Grünberg, Soft Matter **5**, 391 (2009).
[37] T. Kawasaki and H. Tanaka, J. Phys. Condens. Matter **23**, 194121 (2011).
[38] D. Carpentier and P. Le Doussal, Phys. Rev. Lett. **81**, 1881 (1998).
[39] The magnetic susceptibility is determined via the comparison of the pair correlation function with simulations as $\chi = (5.75 \pm 0.05) \times 10^{-11}$ Am^2/T.
[40] F. Ebert, P. Dillmann, G. Maret, and P. Keim, Rev. Sci. Instrum. **80**, 083902 (2009).
[41] K. Binder, Rep. Prog. Phys. **60**, 487 (1997).
[42] D. R. Nelson, in *Phase Transition and Critical Phenomena*, edited by C. Domb and J. L. Lebowitz (Academic, New York, 1983).
[43] See Supplemental Material at http://link.aps.org/supplemental/10.1103/PhysRevLett.111.098301 for an evaluation of simulation data equivalent to Fig. 4, movies illustrating criticallike fluctuations in simulations and experiment, details on the polynomial fit criterion, further evidence for the continuous nature of the phase transition, and an evaluation of spatial correlation functions.
[44] H. Shiba, A. Onuki, and T. Araki, Europhys. Lett. **86**, 66 004 (2009).